Characterization of the Binding Poses of Classical and Photoswitchable Psychedelics Interacting with 5-HT_{2A}R

Vito F. Palmisano,[†,‡] Claudio Agnorelli,[¶,§] David Erritzoe,[¶] Andrea Fagiolini,[§] Shirin Faraji,[*,‡] and Juan J. Nogueira[*,†,‖]

†*Department of Chemistry, Universidad Autonoma de Madrid, Madrid, Spain.*

‡*Theoretical Chemistry Group, Zernike Institute for Advanced Materials, University of Groningen, Groningen, The Netherlands.*

¶*Center for Psychedelic Research, Division of Psychiatry, Department of Brain Science, Imperial College of London, London, United Kingdom*

§*Unit of Psychiatry, Department of Molecular Medicine, University of Siena, Siena, Italy*

‖*IADCHEM, Institute for Advanced Research in Chemistry, Universidad Autonoma de Madrid, Madrid, Spain*

E-mail: s.s.faraji@rug.nl; juan.nogueira@uam.es

Abstract

Classic psychedelics are compounds that target the 5-hydroxytryptamine receptor type 2A (5-HT_{2A}R), inducing profound changes in consciousness. Although these compounds most closely resemble the natural neurotransmitter serotonin, their therapeutic and psychoactive action is still not well understood. Therefore, a quantitative atomistic description of their interaction in the 5-HT_{2A} receptor is required to shed light into their mode of action. In this work, we performed a computational characterization of the orthosteric binding pocket for classical and photoswitchable psychedelics

by means of semi-flexible molecular docking, classical molecular dynamics and binding free energy computations to identify the interactions with the key protein residues. Two nearly degenerate binding poses were observed inside the orthosteric pocket. 5-HT (5-hydroxytryptamine) and LSD (lysergic acid diethylamide) show a preference for the canonical crystallized pose of the 5-HT_{2A}R-LSD structure, in contrast to N,N-DMT (N,N-dimethyltryptamine) and 4-OH-N,N-DMT (4-hydroxy-N,N-dimethyltryptamine), which show a small preference for the newly identified pose. The photoswitchable analogs trans- and cis- AzobenzeneDMT (AzoDMT) interact similarly to N,N-DMT, with the cis-AzoDMT isomer being the most stable. Finally, the azobenzene domain of both cis- and trans-AzoDMT interact with the same key residue (L229) responsible for the extracellular loop closure of LSD. Our simulations clarify the nature of intermolecular drug/protein interactions, which can help to develop new classes of classical and photoswitchable psychedelics.

Introduction

After decades of global constraint on research, the current "renaissance" of scientific interest in hallucinogenic compounds is one of the most promising areas in mental health.[1] Classic psychedelics (meaning "mind-manifesting") are a class of hallucinogenic compounds comprising three main chemotypes: phenethylamines, including mescaline and synthetic substituted phenethylamines (e.g., 4-bromo-2,5-dimethoxyphenethylamine (2C-B), 2,5-dimethoxy-4-iodoamphetamine (DOI), and 4-[2-[(2-hydroxyphenyl)methylamino]ethyl]-2,5-dimethoxybenzonitrile (25CN-NBOH);[2] ergolines, including LSD (lysergic acid diethylamide) and the non-hallucinogenic lisuride and ergotamine;[3,4] and tryptamines, including psilocybin, N,N-DMT (N,N-dimethyltryptamine), and 5-MeO-DMT (5-methoxy-N,N-dimethyltryptamine).[5] Over the last few years, an ever-increasing number of clinical trials is harnessing the potential of psychedelic-assisted psychotherapy to target a variety of internalizing psychiatric conditions, such as addiction, depression, obsessive-compulsive disorder, anorexia nervosa, anxiety, chronic pain, and trauma.[6]

In this context, research has shown that psychedelics can induce significant rapid-acting and long-lasting therapeutic effects, as opposed to typical psychiatric medications that require repeated exposure and have longer onset of action.[7] The precise mechanism of action of these compounds in the brain remains elusive, but evidence coming from different levels of analysis is emerging. Neuroimaging studies in humans have consistently found that during the acute phase, psychedelics increase functional connectivity across typically unrelated brain regions and increase brain signal complexity.[8,9] Another well-replicated finding is the reduction of power in low-frequency brain waves, an effect associated with the emergence of sensory hallucinations.[10] Animal studies have shown that psychedelics induce long-term morphological changes in neurons, leading to an increase in the number of neural branches and synapses.[11] Consistently, psychedelics promote the expression and up-regulation of neuroplasticity-related genes, an effect lasting several days after drug exposure.[12] Importantly, all such changes correlate with the long-lasting therapeutic effects of psychedelics, potentially serving as the structural basis for the rewiring of pathological brain circuitry.

Agonism of the 5-hydroxytryptamine receptor type 2A (5-HT2AR), called 5-HT or serotonin, is thought to be the main mediator of both the subjective and neurophysiological effects of classic psychedelics, although they have complex pharmacological profiles.[13] 5-HT2AR is a canonical G protein-coupled receptor (GPCR), which interacts with various post-synaptic effectors, as schematically shown in Figure 1.

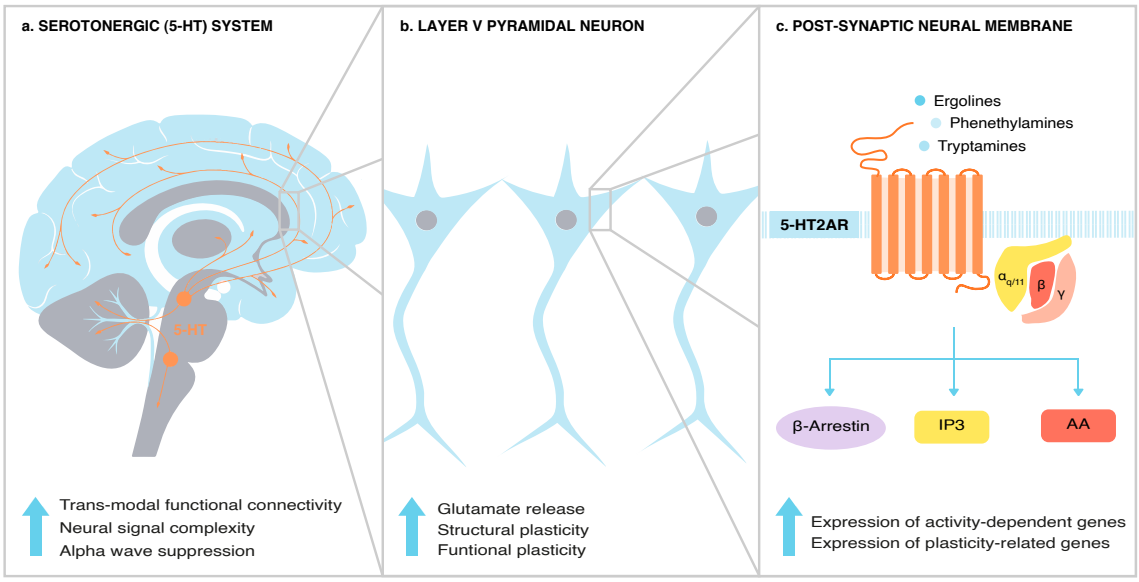

Figure 1: Schematic representation of neurophysiological effects of the interaction of classic psychedelics with the 5-HT system. a) Brain-wide increase in functional connectivity between typically unrelated regions, increase in brain signal complexity, and reduction in alpha wave spectral power. b) Frontocortical release of glutamate and increase in structural and functional plasticity in layer V pyramidal neurons. c) Agonism at the 5-HT2AR, triggering three main post-synaptic signalling cascades via transduction of the G-coupled protein Gq. Those includes the canonical inositol trisphosphate (IP3) pathway, the β-arrestin-2 pathway, and the arachidonic acid (AA) pathway. As a result, there is an increase in the expression of activity-dependent and plasticity-related genes.

In humans, the 5-HT2AR is densely expressed in cortical and neocortical regions involved in cognition, perception, sensorimotor gating, and mood.[14] In particular, the apical dendrites of glutamatergic pyramidal neurons located in the layer V of the prefrontal cortex have a high density of 5-HT2ARs. When stimulated by the endogenous ligand 5-HT and by classic psychedelics, those neurons fire, leading to glutamate release, as represented in Figure 1. Such neuronal activation is mediated by three main molecular pathways, namely the Gq/11, the β-arrestin-2, and the arachinoid acid (AA) pathways, although additional pathways have been found.[15–18] Activation of those signalling molecules leads to an increase of intracellular calcium (Ca^{2+}), causing neuronal firing and expression of activity- and plasticity-related genes. Virtually all psychedelics seem to activate those pathways, as also do the endogenous

ligand 5-HT and some non-hallucinogenic analogs, but there is significant compound-specific variability in the relative signaling potencies and subjective effects those molecules produce. It has been proposed that different agonists can stabilize distinct active conformational receptor states, thus interacting with specific receptor residues to trigger specific subsets of signaling proteins coupled to the receptor, a phenomenon known as "biased agonism".[15,16] Yet, this concept is mechanistically poorly understood, and the study of ligand-receptor interactions in the context of psychedelics is still in its infancy.

The first 5-HT2 family receptor to be crystallized was the 5-HT_{2B}R in complex with ergotamine,[19,20] followed by the 5-HT_{2B}R with the β-arrestin biased LSD.[21] In the last few years, several new 5-HT2 structures were crystallized: The inactive structure of 5-HT_{2C}R[22] and 5-HT_{2A}R,[23,24] the G-αq-coupled active structure of 5-HT_{2A}R[24] and, very recently, the lipid activated structure of 5-HT_{2A}R.[25] Based on those results and previous site-directed mutagenesis studies, the orthosteric binding pose (OBP) of the 5-HT_{2A}R has been identified and characterized.[26,27] Yet, the bound structure to its endogenous compounds, 5-HT and N,N-DMT, is not available, but the 5-HT_{2A}R-LSD bound structure may provide hints about the binding mode of the indole moiety shared between ergotamines and tryptamines, and unravel, at the atomistic level, the extremely different pharmacological output induced by biased agonism.[28]

In addition to the multivariable problem of biased agonism, drug selectivity is a major problem of classical pharmacology, originated by uncontrolled drug activity in time and space. To this end, photopharmacology, allows to reversibly photosensitize an exogenous compound, and control its activity via illumination in the UV-vis region, recently opening its application to in vivo studies.[29] The main benefit of photopharmacology strategies is that they enable to follow a drug with a high spatio-temporal resolution, retaining the biological activity ("on") in at least one of the conformations and be non-toxic in the other one ("off"), reducing the off-target side effects and decreasing drug resistance.[30] After its

full establishment into class A rhodopsins,[29] which incorporates a class of photoreceptors,[31] recently, a series of photoswitchable ligands for optical control of the 5-HT_{2A}R based on the endogenous compound 5-HT was synthesized and tested.[32] The lead compound, Azo-5HT-2 is inactive in the dark state and showed preferential agonism upon illumination in the UV region. In addition, a very promising class of photoswitchable agonists of the 5-HT_{2A}R based on the structure of N,N-DMT was created, tackling the C4-C6 position of the indole group, optimizing the size of the molecule by incorporating only one aromatic ring. One of the compounds emerged as a cis-on "efficacy switch" at 385 nm and allowed reversible optical control of 5-HT2AR.[33]

Despite these promising results shown by photoactivatable drugs, no mechanistic studies investigating at atomistic level the binding mode of photoswitchable agonists in the 5-HT_{2A} receptor, and the main differences with the binding of classical psychedelics, are available. In this context, the performance of computational studies is a fundamental tool since the identification of the key protein residues involved in the binding process of the photosensitive domain would allow for a selective functionalization of the aromatic rings of the drugs and for a better understading of the mode of action of the 5-HT_{2A}R protein control. Herein, we characterize the binding mode of different drugs into the 5-HT_{2A}R protein by means of semi-flexible molecular docking, classical molecular dynamics (MD) simulations, and molecular mechanics generalized Born surface area (MMGBSA) free energy calculations. Specifically, 5-HT, N,N-DMT, 4-OH-DMT (4-hydroxy-N,N-dimethyltryptamine), LSD and the azobenzene (Azo) based photoswitchable analogs of the psychedelic compound, trans-Azo-N,N-DMT and cis-Azo-N,N-DMT, based on the structure of trans-Azo-5HT-2,[32] are investigated (see Figure 2a).

Computational Details

Molecular Docking

The crystal-bound structure of the 5-HT_{2A}R with the partial agonist LSD was obtained from the RCSB-PDB (PDB ID: 6WGT).[24] The ligands 5-HT, N,N-DMT, 4-OH-DMT, LSD and cis/trans-Azo-N,N-DMT (Figure 2a) were constructed using IQmol Molecular Viewer.[34] The geometry of the ligands was optimized at B3LYP/cc-pVDZ level of theory, and the ESP Merz-Singh-Kollman charges were obtained from the optimized structure at HF/6-31G* level of theory with Gaussian09 software.[35] Protein and ligand preparation and docking were completed using AutoDock Vina,[36] which added polar hydrogens, united atom Kollman charges, solvation parameters and fragmental volumes to the protein. Protonation states were assigned with Open Babel with a target pH of 7.4.[37] The grid size was set to 20 x 20 x 20 xyz points with a grid spacing of 1 Å, centered at the orthosteric binding pose. During the docking simulation, the protein was considered to be rigid, while the ligands were considered flexible. For the photoswitches, the C-N=N-C and C-C=N-N dihedral angles were locked to their equilibrium values to avoid torsion during the sampling. In this way, we are able to discriminate between the two isomers' binding modes, in case they differ.

Since the orthosteric binding pose for 5-HT and N,N-DMT was characterized in previous mutagenesis studies[38–43] and LSD was recently crystallized in 5-HT_{2A}R,[24] the docking poses were selected based on those findings. In particular, the orthosteric binding pose presents the following features: the protonated primary/tertiary amine nitrogen of the drug interacts with D155, the indole -N1 atom creates a hydrogen bond with S242, and the aromatic indole group interacts with W336, F339 and F340 via hydrophobic interactions (Figure 2b,c). During the MD simulation of 5-HT (see below), the indole group performed a ≈180° rotation along the C2 bond (see Figure 2a), showing a new binding pose where the key interactions are retained but the indole group points towards the inside of the pore, into a hydrophobic cage formed by W336, F339 and F340 (Figure 3a). A representative snapshot of the protein

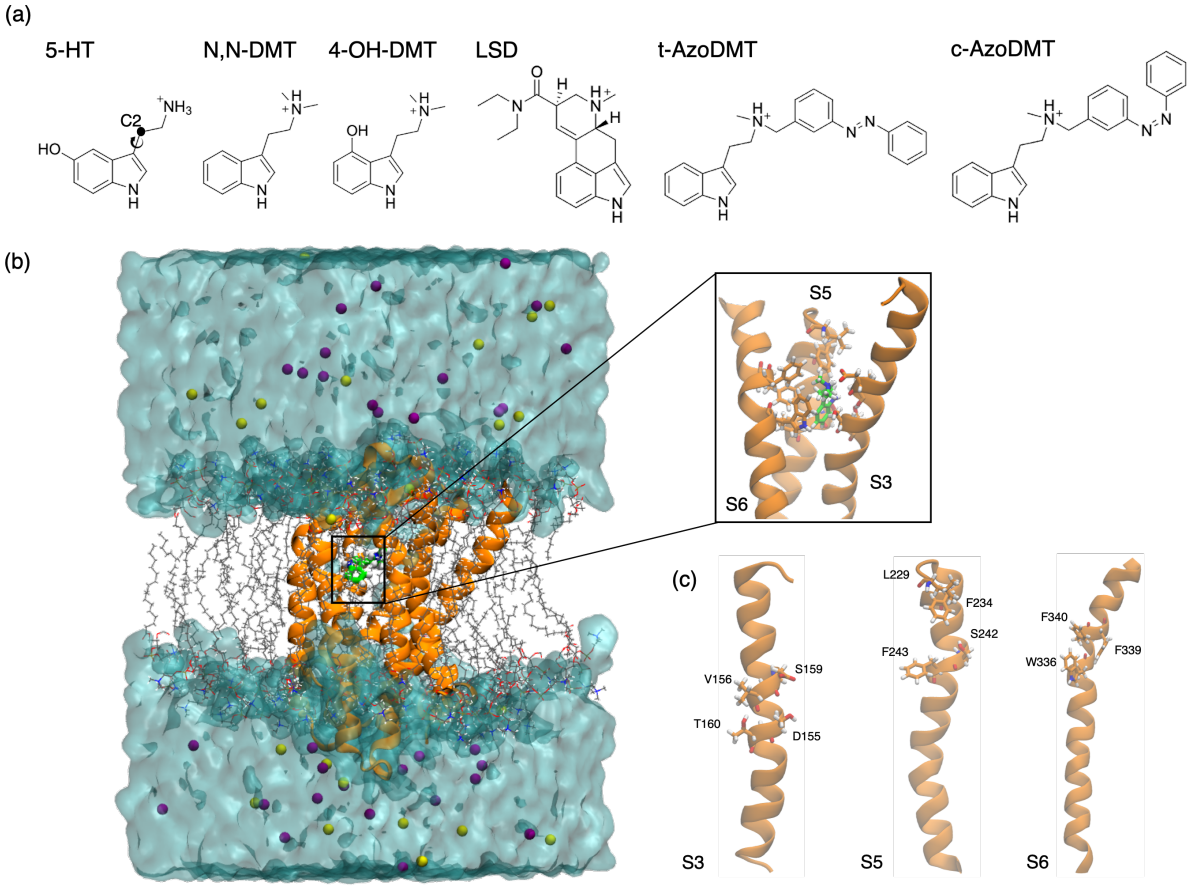

Figure 2: (a) All the compounds under investigation. (b) Representation of N,N-DMT (green) interacting with the 5-HT_{2A}R (orange) embedded into a membrane (gray). Water is represented by the cyan surface and the Na^+ and Cl^- ions by the yellow and violet beads. The black rectangle shows a simplified zoom of the OBP including a portion of the S3, S5 and S6 helices interacting with N,N-DMT. (c) Cartoon representation of the S3, S5 and S6 helices with a licorice representation of the residues involved in the major interactions with N,N-DMT.

was extracted from the simulation and used again for semiflexible docking using the same procedure, to dock the tryptamines and LSD to the newly discovered binding pose. A total of 12 binding poses, two per each compound (p_1 and p_2) were selected as initial structures to run MD simulations, where p_1 represents the pose discovered via MD simulations, while p_2 represents the canonical binding pose of the 5-HT_{2A}R-LSD bound structure.

Molecular Dynamics System Setup

Missing heavy atoms and hydrogens were added with the tleap module of the Amber20 package for the 5-HT_{2A} receptor.[44] The protein-ligand complexes obtained from docking were aligned along the z-axis using the Positioning of Proteins in Membrane (PPM) web server.[45] The complexes were then inserted in a 1-palmitoyl-2-oleoyl-sn-glycero-3-phosphocholine (POPC) lipid bilayer (xy length: 50 x 50 lipid components), and solvated in a rectangular box with aqueous solvent and NaCl at a concentration of 0.15M L^{-1} (box dimensions: x: 67.9 Å, y: 67.9 Å, z: 109.9 Å) with the CHARMM-GUI Bilayer Builder.[46] Potential parameters for the protein, lipids, water and ligands were taken from the FF19SB, Lipid17, TIP3P and GAFF2, respectively.[47–50] For the two isomers, trans-AzoDMT and cis-AzoDMT, dihedral parameters were taken from the GAFF2 with the exception of C-N=N-C and C-C-N=N, which were taken from a previous work.[51] In total, the solvated systems were composed by $\approx$ 45000 atoms.

Classical Molecular Dynamics Simulations

Classical MD simulations for the solvated membrane-protein-ligand system were performed with the CUDA version of the AMBER20 package.[44,52] First, energy minimization was carried out with the steepest descent method for 5000 steps followed by the conjugate gradient method for additional 5000 steps. Positional restraints were applied to the membrane-protein-ligand system gradually from 10 to 1 kcal/(mol $Å^2$), while heated from 0 to 303.15 K with the Langevin thermostat for a total of 120 ps. The desired density was reached by run-

ning an equilibration in the NPT ensemble with a Monte Carlo barostat and a semiisotropic pressure scaling for 4 ns. For 5-HT, N,N-DMT, 4-OH-DMT and LSD, an unconstrained production run was carried out at 303.15K for 200 ns, while for trans/cis-AzoDMT it was carried out for 500 ns. During the full MD protocol, a timestep of 2 fs was employed, the cutoff radius and switching distance to compute the non-bonded interactions were set to 12.0 Å and 10 Å, respectively, and bond lengths involving hydrogen atoms were kept fixed using the SHAKE algorithm.[53,54]

MMGBSA free energy analysis

The binding free energy of all the systems was calculated with the one-average molecular mechanics generalized Born surface-area (1A-MM-GBSA) approach.[55] From the most stable 100 ns interval of the production run, in terms of the root mean squared deviation (RMSD) of the drug, 1000 equidistant snapshots were selected to calculate the MMGBSA total binding free energy. In addition, a pairwise residue free-energy decomposition analysis was performed to obtain the contribution of each residue-ligand interaction to the total binding free energy. The decomposition was performed by considering residues within a radius of 5Å distance from the ligand.

Results and Discussion

Classical Psychedelics

Total Binding Free Energy

As explained above, the docking and MD simulations found two different poses (p1 and p2) for the drugs inside the orthosteric binding pocket of the receptor (Figure 3a). During the MD simulations, both poses were stable for all the ligands, as can be concluded from the time evolution of the RMSD of the drugs shown in Figure 3b. However, the p2 pose displays

relatively large RMSD oscillations for the cis and trans forms of the AzoDMT compound. The visualization of the trajectories revealed that this is a consequence of the motion of the azobenzene moiety of the photoswitchable drug, which interacts in a weaker way with the protein than the indole fragment.

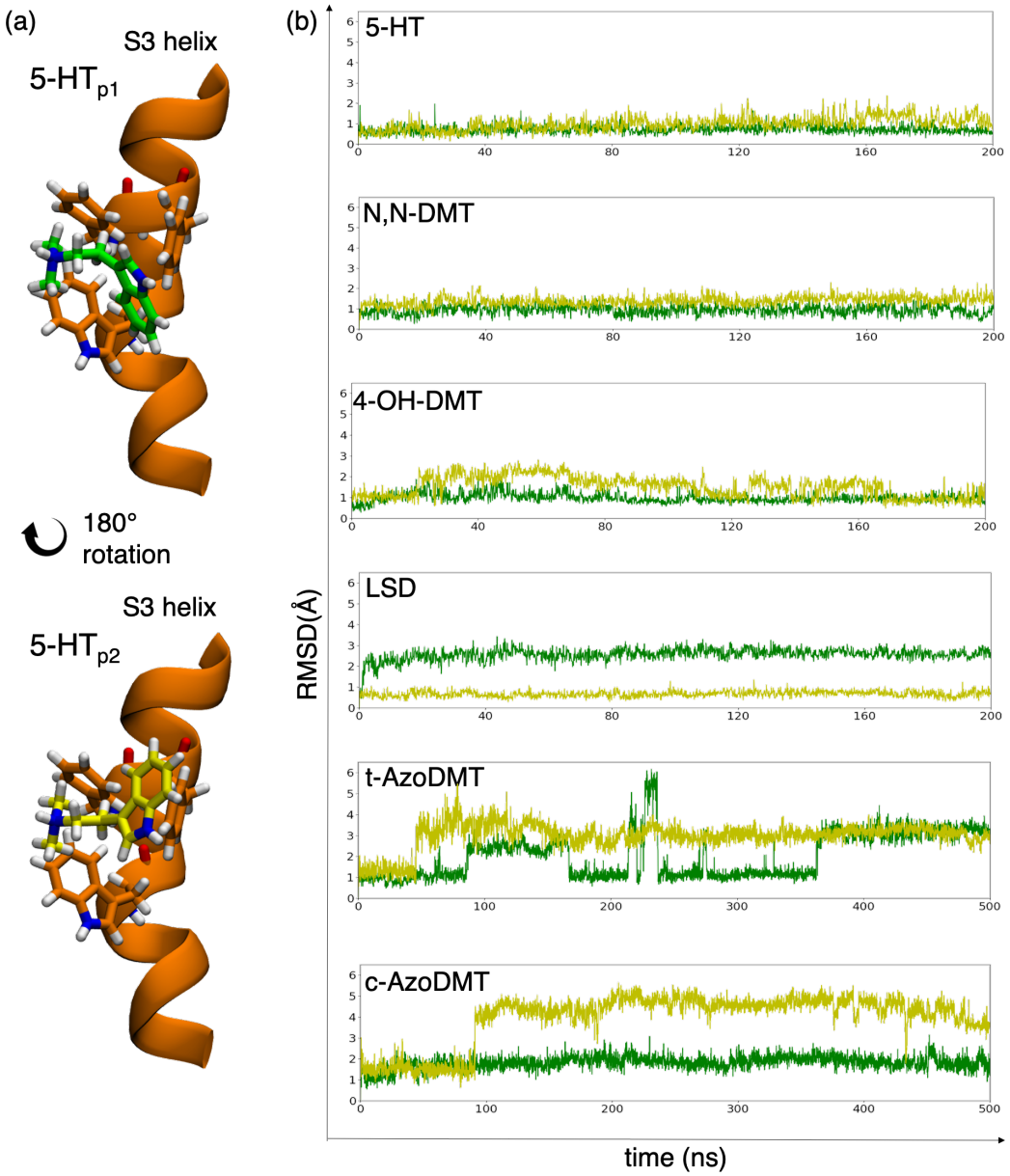

Figure 3: (a) Representation of N,N-DMT interacting with the S3 helix showing the 180 rotation along the C2 carbon. (b) RMSD of 5-HT, N,N-DMT, 4-OH-DMT, LSD for 200ns and of t-AzoDMT and c-AzoDMT for 500ns of production run. The green and yellow lines represent the p_1 and p_2 poses respectively.

The ligand/protein binding free energy was computed by the 1A-MM-GBSA approach by considering 100 ns from the dynamics. Then, it was decomposed into electrostatic, van der Walls, and solvent polar and non-polar contributions. The energies for the classical psychedelic drugs (not the photoswitchable ones) are shown in Figure 4. Overall, all the compounds present similar energies but LSD in the p2 pose, which displays the lowest total binding free energy of -63.7 kcal/mol. It should be highlighted that the higher binding free energy found for LSD results from additional interactions of its diethylamide domain, further discussed in the next section, which is not present in the other drugs.

Looking at the interaction types involved in the binding (Figure 4), the electrostatic contribution is larger for 5-HT than for the other compounds. In 5-HT, the presence of the 5-OH, indole -NH, and protonated primary amine groups provide five hydrogen bond (HB) donor atoms, as opposed to the protonated tertiary tryptamines, which have only two (N,N-DMT and LSD) and three (4-OH-DMT) HB donor atoms. However, those tertiary tryptamines present a higher van der Waals contribution than 5-HT. Despite their analogous structures, the ligands do not share the same lowest energy binding pose (Figure 4). 5-HT and LSD show an energy difference between the two poses of -5.5 and -16.1 kcal/mol, respectively, in favor of the canonical p_2 pose. The p2 is favored in 5-HT due to the stronger van der Waals interactions than in p1, while in LSD p2 is more stable than p1 due to the electrostatic contribution. The tertiary tryptamines, N,N-DMT and 4OH-DMT, on the other hand, favor the binding to the hydrophobic p_1 pose. However, in those cases, the stability of the different poses relies on a complex balance among all the energy terms. N,N-DMT_{p1} and 4-OH-DMT_{p1} display a higher van der Waals energy (in absolute value) and a lower polar energy compared to N,N-DMT_{p2} and 4-OH-DMT_{p2}. This can be understood when analyzing the protein residues interacting with the drug in each of the poses (Figure 5a,b). In p1, the aromatic indole and the dimethyl amine groups are locked into a hydrophobic cage formed by several highly conserved aliphatic and aromatic residues, which favor the formation of non-polar interactions, e.g., $\pi - \pi$ interactions, which are classified as van der Waals inter-

actions in the force field employed here. In addition, the energy penalty associated with the desolvation of the residues is lower in the p1 pose because of their more hydrophobic nature.

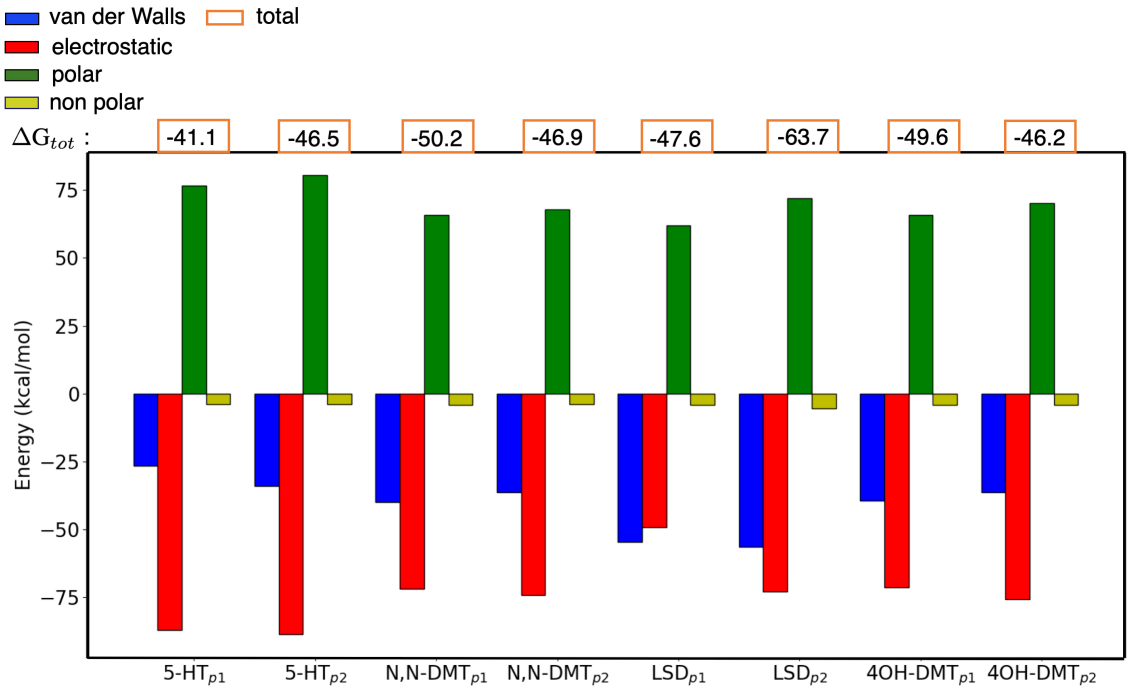

Figure 4: Total free energy (orange squares) in kcal/mol and its decomposition into van der Walls (blue), electrostatic (red), polar (green) and non- polar (yellow) for all the classical psychedelics.

The next section will provide a more detailed discussion of the residues involved in the binding of all the compounds. First, a description of the canonical p_2 pose is discussed. Then, a comparison between p_1 and p_2 for the classical tryptamines and LSD is performed to understand the main dissimilarities between the two poses. Finally, the binding modes of the photoswitches are described and the interactions with the key residues are compared to the non-photosensitive compounds.

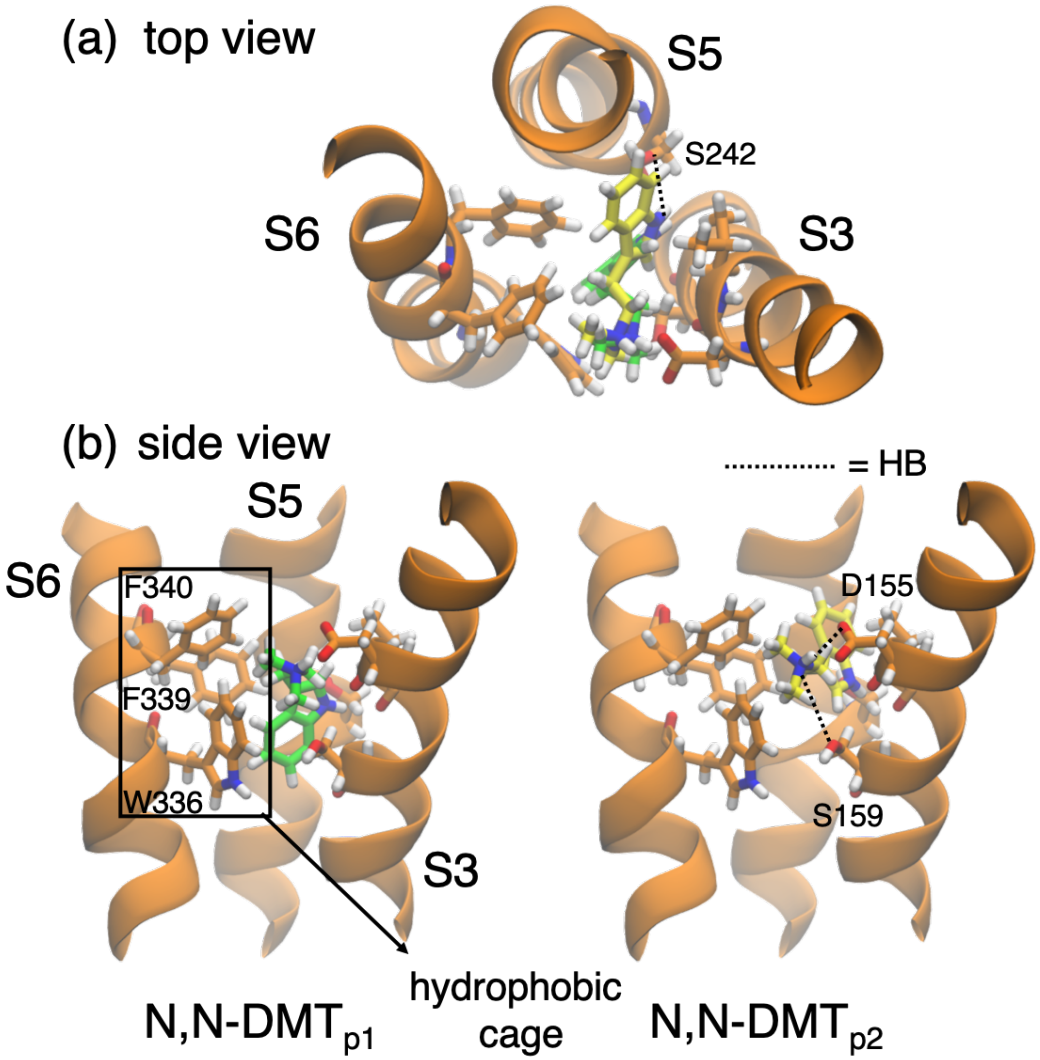

Figure 5: (a) Top view of the OBP with N,N-DMT$_{p1}$(yellow) and N,N-DMT$_{p2}$ (green). (b) Side view of the OBP with DMT$_{p1}$ (yellow) and N,N-DMT$_{p2}$ (green).

The Canonical p_2 Pose

The canonical OBP is located ≈10 Å inside the 5-HT$_{2A}$R protein from the extracellular medium, with the helices S3, S5 and S6 folding towards the center of the pore, resulting the most involved protein fragments in the binding of the drugs, as shown in Figure 5. All the ligands under investigation have been docked to the OBP with the same tryptamine orientation. Figure 6 illustrates with a heat-map the pairwise residue-ligand decomposition

of the total binding free energy for each classical ligand in the p_1 and p_2 pose.

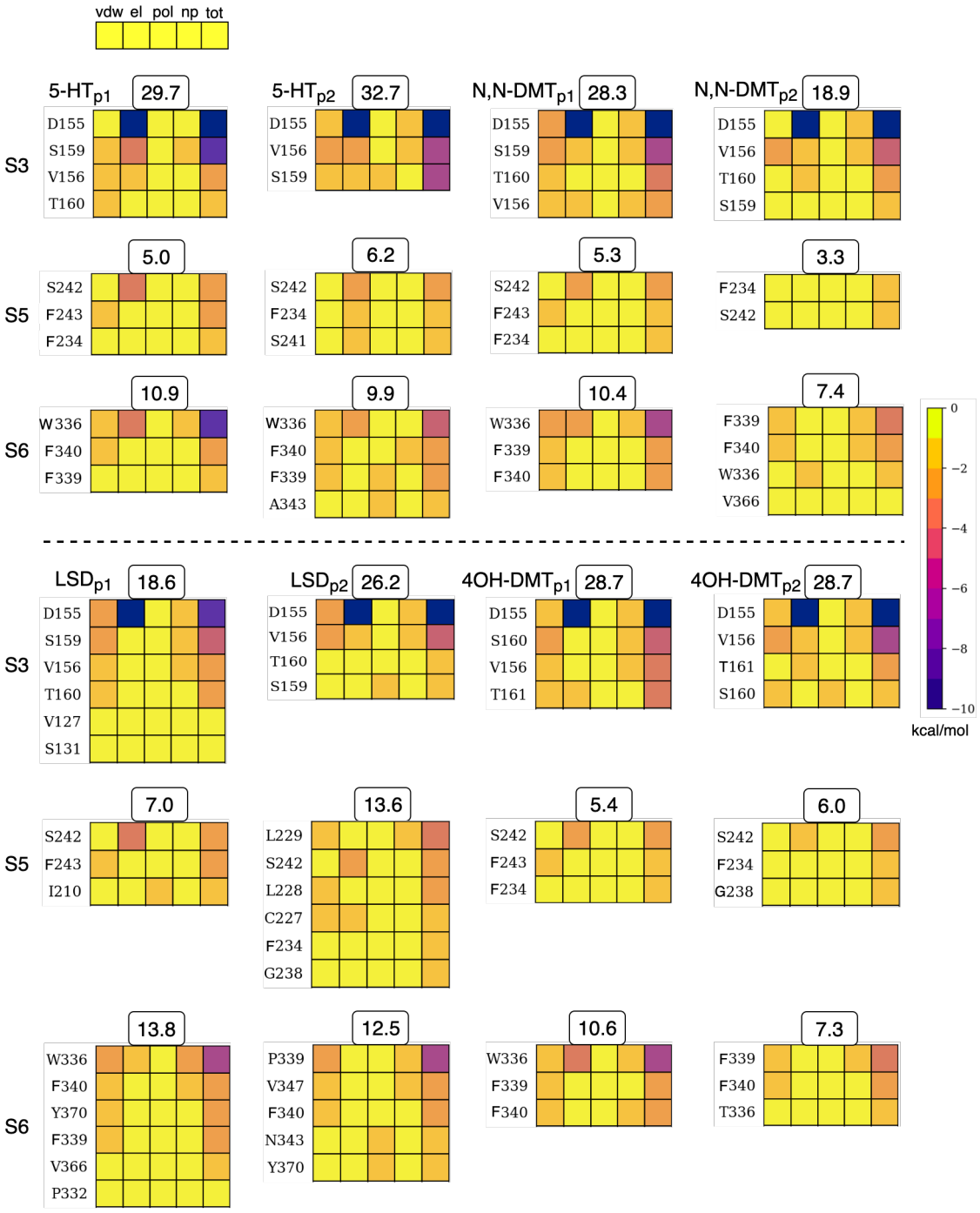

Figure 6: Pairwise residue decomposition of the binding free energy for the p1 and p2 poses of 5-HT, N,N-DMT, LSD and 4-OH-DMT. Each residue contribution is in turn decomposed into ligand/protein van der Walls (vdW) and electrostatic (el) contributions and polar (pol) and nonpolar (np) solvation contributions to the total residue binding energy (tot). The rectangle on top of each heat-map represents the total energy of interaction in kcal/mol (in absolute value) between the helix and the ligand.

The S3 helix, accommodates the alkylamine domain of all the compounds, with D155 being the major contributor to the anchoring of the alkylamine to the pose. 5-HT, N,N-DMT, LSD and 4OH-DMT (mainly protonated at physiological conditions) form salt bridges interactions between their $^{+}NH_3$ and $^{+}NH(CH_3)_2$ groups and the negatively charged side chain COO^- of D155. This residue contributes ≈40% to the total binding free energy for 5-HT, N,N-DMT, LSD and 4OH-DMT, ranging between -18.0 and -22.0 kcal/mol (Figure 6). Experiments revealed that the D155A, D155Q and D155N mutations of the 5-HT_{2A}R protein completely disrupt the binding of both 5-HT and N,N-DMT, but upon the D155E mutation N,N-DMT affinity is higher, showing that the longer alkyl chain of glutamic acid can substantially change the affinity of the drug, mainly because of steric effects.[38,43]
Moving along the S3 helix, V156 has equal importance for all compounds, since it interacts via its isopropyl side chain with the aromatic indole and via HB with the -N1 indole. This residue was never mutated but it was previously mentioned to be a strong contributor to the binding of 25X-NBOMEs and LSD.[56] Finally, S159 interacts with 5-HT, N,N-DMT, 4OH-DMT and LSD through HB between its -OH side chain and the primary/tertiary alkyl amines of the drugs. For the primary amine compound, 5-HT, a much stronger interaction is observed due to a larger number of HB sites available in comparison to the other compounds. In fact, the S159 residue was intensively studied via mutagenesis to understand the change in binding affinity of 5-HT, N,N-5-HT and LSD between the native and the S159A mutants. It was shown that 5-HT substantially decreases its affinity by the S159A mutant, while only shows an intermediate decrease in affinity for the S159C variant. In contrast, N,N-5-HT showed no decrease in affinity by the S159C mutation and a very small decrease by S159A results,[41] fully in agreement with the current. This is the first energetic difference observed in S3 between the primary amine 5-HT and the tertiary amine compounds. Overall, S3 is the helix that provides the strongest interactions, which are mainly of electrostatic character with the alkylamine domain, as observed in Figure 6.

In the S5 helix, S242 is the main contributor to the binding energy (see Figure 6), which

interacts with its -OH side chain with the indole -N1 of all compounds via HB. Interestingly, rodents 5-HT_{2A}R possess a A242 at the human's S242 position, and A242S mutation in rodents resulted in a pharmacological profile almost identical to that of the human.[57,58] In addition, it was previously demonstrated that -N1 substitution of the ergolines and tryptamines have no effect in the affinity to 5-HT_{2A}R receptors in rodents. In contrast, N1-alkyl substitution of the same ergolines and tryptamines results in a substantial difference in affinity for the pig, squirrel, monkey and human proteins.[59] For the more extended ergotamine molecule, LSD, further stabilization is achieved with the alkylamide domain that creates HB with C227, hydrophobic interactions with L228 and, particularly, with L229, which is the strongest contributor to the binding in S5, in agreement with the crystallized structure of 5-HT_{2A}R-LSD.[24] LSD_{p2} in fact shows the strongest interaction with S5, in comparison to all the other compounds (Figure 6).

The S6 region involved in the OBP is mainly hydrophobic and stabilizes the interaction with the ligands via cation-π and π-π interactions with the indole group of tryptamine and ergotamine molecules. Mainly, three aromatic residues contribute to the binding of 5-HT, N,N-DMT, 4-OH-DMT and LSD: W336, F339 and F340. The W336 is the major contributor to the binding energy in 5-HT, while is weaker in N,N-DMT, 4-OH-DMT and LSD. In the simulation, 5-HT mainly binds via a cation-π interaction with W336, giving raies to a large electrostatic contribution. W336 has been proposed for many years as a "toggle switch" that controls GPCRs transitioning between inactive and active state.[60] The F340 residue shows a T-shaped $\pi\pi$ interaction with the indole aromatic group, and the van der Walls term predominates in the interaction. In fact, mutagenesis studies showed that F340L mutation greatly diminishes the affinity of a series of 5-HT_{2A}R agonists including 5-HT and 5MeO-N,N-DMT. However, the F340Y mutation behaved identically to the native receptor showing that an aromatic residue is required at that position, but not specifically phenylalanine.[40,61] Finally, LSD weakly interacts also with N343, V366 and Y370.

The p_1 versus p_2 Binding Poses

During the MD simulation of 5-HT_{p2}, the indole group performed a ≈180° rotation along the C2 bond (Figure 3a) going to the p1 pose, allowing the ligand to retain the interactions with the key residues of the initial p2 pose, but with slightly different strength. Even though the spatial orientation of the tryptamine domain is the same for 5-HT, N,N-DMT, 4-OH-DMT and LSD, the compounds showed different preferences towards the p_1 and p_2 poses, where common interactions are retained with S3, S5 and S6 helices (see Figure 6).

Starting from S3, the first difference between the two poses is found at the interaction with V156, which creates strong van der Waals interactions of its isopropyl side chain with the indole group in the p_2 pose, which are in a more favorable orientation for alkyl-π interaction. Instead, S159 interacts in a stronger fashion with the drugs in the p_1 pose, since their orientations in the S3 helix favors van der Waals interactions with the indole group of the four compounds in addition to the HB created with the alkylamine domain, which is pronounced in 5-HT, due to the larger amount of HB sites available. An exception is observed for LSD, where the difference between the two poses is determined by the interactions with D155, being -7.8 and -18.6 kcal/mol for p_1 and p_2 respectively. The ergotamine LSD must be thought of as a rigid tryptamine, therefore the rotation of the cyclic domain implies also a rotation of the alkylamine, which then disfavors the interaction with D155, in contrary to classical tryptamines, where the indole group can freely rotate along the C2 carbon, without perturbing the alkylamine interaction.

The total binding free energy with the S5 helix ranges between -5 and -7 kcal/mol for all the ligands, with the exception of LSD, which presents a stronger interaction. Both binding poses create an HB with S242 and a T-shaped π-π interaction with F234. LSD_{p2} creates, in addition, an essential hydrophobic interaction with L229 through the alkylamine domain, which is the main contributor to the binding free energy in S5. The L229 residue was previously observed to work as an extracellular "lid" both in 5-HT_{2B}R (L209) and 5-HT_{2A}R, increasing the resistance time of the drug.[21] This effect is observed in the LSD_{p2}

simulation, where the isopropyl group of L229 interacts with the ligand and induces a loop closure at the extracellular region.

The S6 helix forms a hydrophobic cage for the indole domain and the dimethylamine group, in the case of N,N-DMT and 4-OH-DMT. The major contributors to the binding, in both poses, are W336, F339 and F340, which contribute with different strengths to the binding depending on the rotation of the indole group in the two poses. First, comparing 5-HT with N,N-DMT and 4-OH-DMT, the major difference in p_1 is the lack of alkyl-π interactions between the dimethylamine and W336 and F339, which is replaced by a strong cation-π interaction in the case of the monoamine 5-HT. The tertiary tryptamine compounds are more hydrophobic and can accommodate better in the cage, in comparison to 5-HT, a fact which is observed in the larger van der Waals energy value and lower polar solvation energy. This is a crucial point because the S6 helix provides the largest structural deformation. Thus, future computational studies should be aimed at investigating these interactions at a QM level, for example, with energy decomposition analysis[62] based on quantum mechanical calculations.

Comparing N,N-DMT and 4-OH-DMT in p_1, the extra hydroxyl group further stabilizes the interaction with W336. In the p_1 pose, all the ligands under investigation interact via T-shaped $\pi - \pi$ stacking with W336 and F340 with the indole group, and via cation-π interactions with F339, as shown in Figure 5. The interaction with the W336 residue is the main contributor to the binding energy. Hoever, for the p_2 pose the interactions with W336 are weaker since the rotation of the indole group disfavors cation-π and $\pi - \pi$ interactions, while the relative distance and orientation to F339 and F340 are retained and become the major contributors.

Overall, despite the similar binding mode and free energy, major differences are observed between the p_1 and the p_2 poses. In the helix S3, where electrostatic interactions dominate, all the compounds strongly interact with the anchor D155, but V156 and S159 determine the binding free energy difference among the different compounds with the helix. In S5,

the main interaction observed for all the compounds is of electrostatic character with S242, except for LSD_{p2}, where the diethylamide domain binds to L229 inducing a loop closure at the extracellular region. Furthermore, in the hydrophobic S6 helix, the residue W336 displays the largest difference in binding free energy between the two poses.

AzoDMTs - Photoswitchable Psychedelics

A photoswitchable analog of N,N-DMT, named here AzoDMT, was analyzed in the two poses (p_1, p_2) in the trans and cis configuration. Both isomers remained bound throughout the full MD simulation, with the tryptamine domain retaining the same interactions as the classical psychedelics. The cis-AzoDMT dissociates from the canonical p2 pose and binds in an additional pose that does not resemble the canonical pose of the classical tryptamines and is not further discussed.

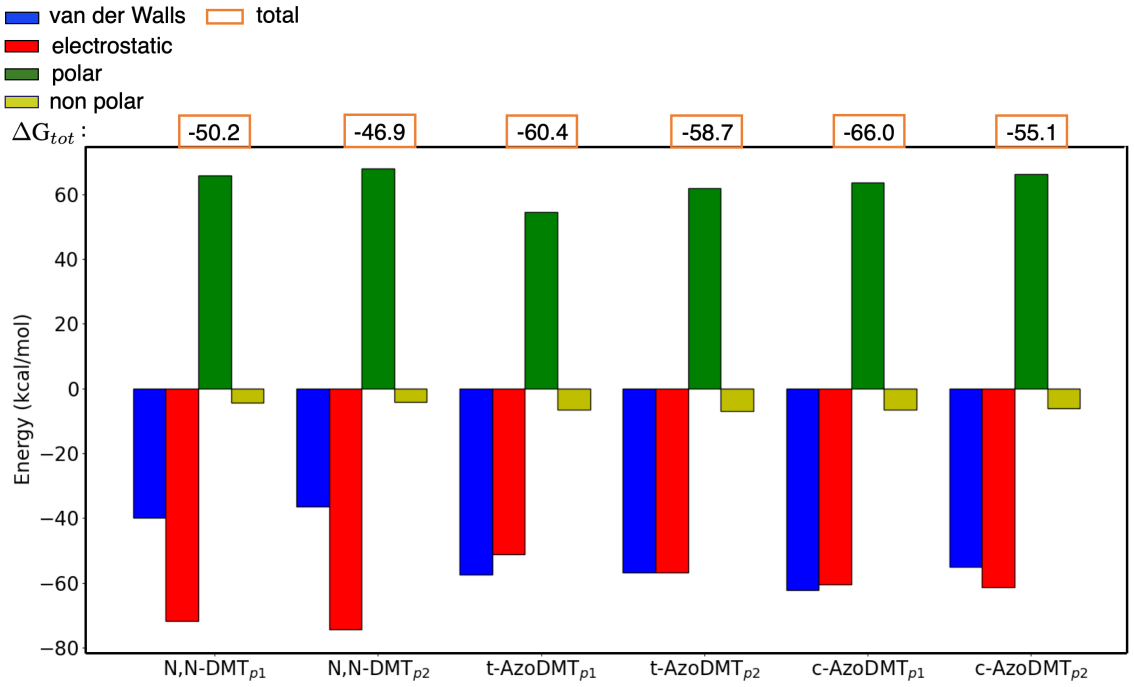

Figure 7: Total free energy in kcal/mol (orange squares) decomposed into van der Walls (blue), electrostatic (red), polar (green) and non polar (yellow) for N,N-DMT and its photoswitchable analogs t-AzoDMT and c-AzoDMT.

As for N,N-DMT, p1 is the most favorable pose for cis-AzoDMT (-66 kcal/mol) and

trans-AzoDMT$_{p1}$ (-60.4 kcal/mol), as can be seen in Figure 7. Interactions at the S3 helix are retained (see Figure 8), with D155 being the anchor of the tertiary amine also for the photoswitches, forming the previously discussed salt bridge between the $^{+}NH(CH_3)_2$ group and the COO^{-} group of the aminoacid. Interactions of electrostatic character with S159 are also maintained in both isomers, while hydrophobic interactions with the isopropyl group of V156 are stronger for the cis isomer since the aromatic rings of the Azo domain bend towards the S3 and S5 subunits. In fact, in addition to the standard HB interaction between S242 and the -N1 indole atom, the photoswitch in the p_1 pose interacts with V235 and F243, and more importantly, hydrophobic interactions are observed with L229, mimicking the loop closure induced by LSD, due to a similar orientation of the Azo domain compared to the diethylamide domain of the psychedelic ergotamine. In the hydrophobic helix S6, interactions with W336, F339 and F340 are also maintained with the same strength as in the tryptamines.

Overall, the Azo moiety orients differently in space between the cis and trans configurations. The trans-AzoDMT extends its Azo moiety towards the extracellular domain, while in the cis-Azo it remains closer to the binding site since it is ≈7 Å shorter in length. It is not possible to argue with the current atomistic simulations whether these two isomers would induce two different molecular signaling and biased agonism, but it is a good starting point for understanding the binding modes of AzoDMTs in the 5-HT$_{2A}$R and functionalizing the Azo aromatic rings on the basis of the ligand-residues interactions. In an ideal case, the two isomers should bind with a completely different mode, in order to induce different pharmacological responses.

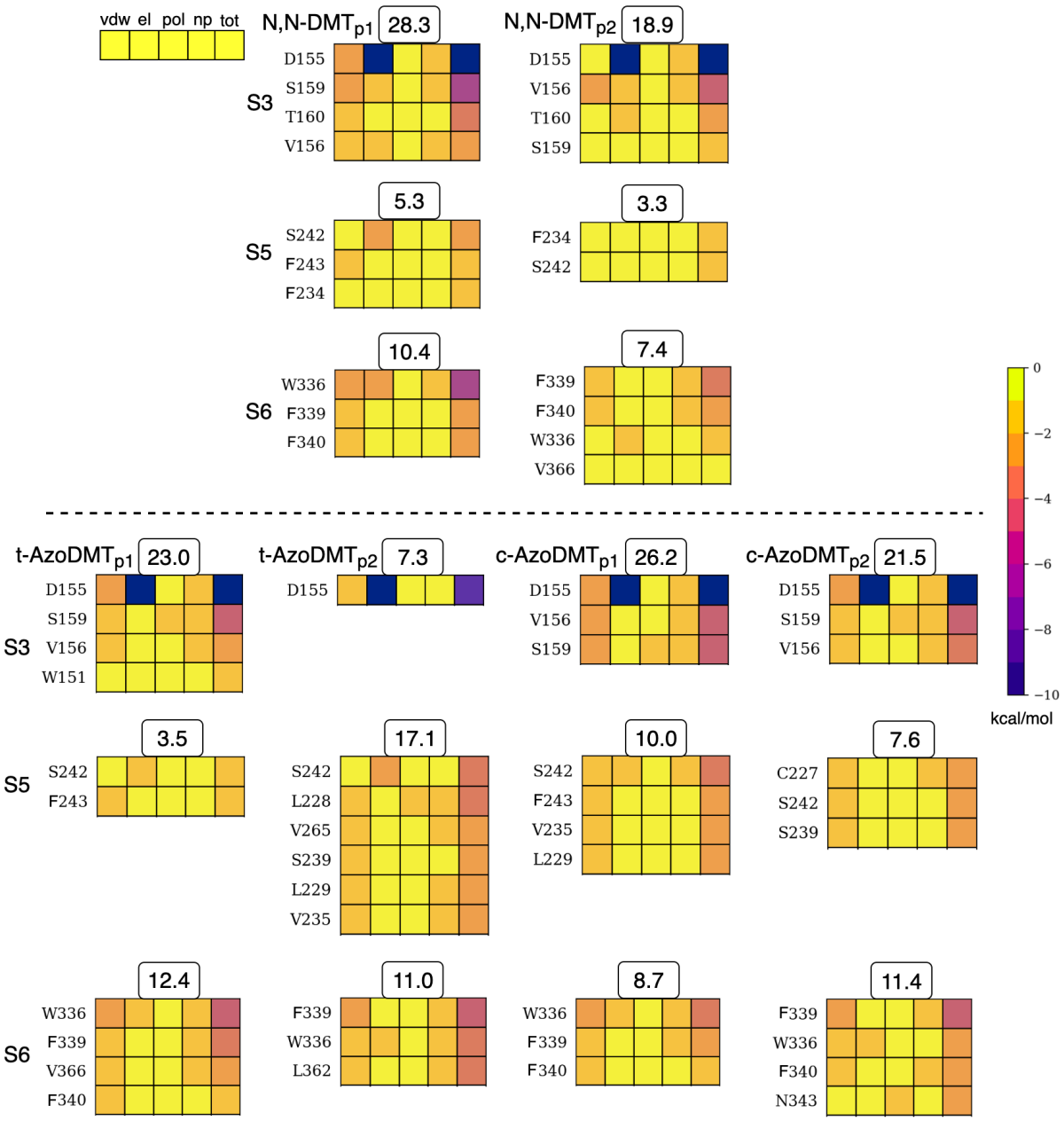

Figure 8: Pairwise residue decomposition of the binding free energy for the p1 and p2 poses of N,N-DMT, trans- and cis- AzoDMT. Each residue contribution is in turn decomposed into ligand/protein van der Waals (vdW) and electrostatic (el) contributions and polar (pol) and nonpolar (np) solvation contributions to the total residue binding energy (tot). The rectangle on top of each heat-map represents the total energy of interaction (in absolute value) between the helix and the ligand.

Conclusions

In the present work, the binding poses of 5-HT, N,N-DMT, 4-OH-DMT, LSD and AzoDMTs in the orthosteric binding pocket of the recently crystallized 5-HT_{2A}R bound to LSD are identified with semi-flexible molecular docking and MD simulations of the ligand-protein complexes embedded in a solvated lipid bilayer. The total binding free energy of the two binding poses is then computed by means of MMGBSA, and the key residues are identified. 5-HT and LSD shows a preference for the canonical p_2 pose, in agreement with the 5-HT_{1A}R bound to 5-HT, while the two binding poses of the psychedelic compounds N,N-DMT and 4-OH-DMT are almost degenerate, with a small preference for p_1. The LSD simulations are in good agreement with the experimetal HT_{2A}R LSD bound structure, since a difference of 16 kcal/mol is observed in favor of the p_2 pose, which was the crystalized one.

Since no crystal structures of 5-HT_{2A} bound to N,N-DMT or other tertiary tryptamine derivatives are available, this is the first atomistic indication of a different binding mode in comparison to the neurotransmitter 5-HT. Finally, the photoswitchable analog AzoDMT, in both trans and cis isomers, favourably binds to the protein with the tryptamine domain interacting similarly to the N,N-DMT ligand. The cis-AzoDMT isomer in the p1 pose was found to be the most most stable situation. In addition, the Azo domain of both cis- and trans-AzoDMT interacts with the same key residues as the diethylamide domain of LSD, therefore they may also mimic the pharmacological effect of ergotamines.

In conclusion, our findings help to clarify the intricate ligand-receptor interactions that form the cornerstone of psychedelics' mechanism of action. This is a first step towards a better understanding of the binding mechanism, which could contribute to the design of new photopharmacological drugs.

Acknowledgement

This work was partially supported by the Spanish Ministry of Science and Innovation through the project PID2020-117806GA-I00 funded by MCIN/AEI/10.13039/501100011033. J.J.N. and V.F.P. acknowledge the Comunidad de Madrid for funding through the Attraction of Talent Program (Grant ref 2018-T1/BMD-10261). S. F. is grateful to Innovational Research Incentives Scheme Vidi 2017 with project number 016.Vidi.189.044, which is partly financed by the Dutch Research Council (NWO).

References

(1) Nutt, D.; Erritzoe, D.; Carhart-Harris, R. Psychedelic psychiatry's brave new world. *Cell* **2020**, *181*, 24–28.

(2) Shulgin, A. T.; Shulgin, A. *PIHKAL: a chemical love story*; Transform Press Berkeley, 1995.

(3) Hofmann, A. How LSD originated. *Journal of Psychedelic Drugs* **1979**, *11*, 53–60.

(4) Shulgin, A. *Psychotropic Agents*; Springer, 1982; pp 3–29.

(5) Shulgin, A. T.; Shulgin, A. *TIHKAL: the continuation*; Transform Press Berkeley, CA, 1997; Vol. 546.

(6) Rucker, J. J.; Iliff, J.; Nutt, D. J. Psychiatry the psychedelic drugs. Past, present future. *Neuropharmacology* **2018**, *142*, 200–218.

(7) Nutt, D.; Spriggs, M.; Erritzoe, D. Psychedelics therapeutics: What we know, what we think, and what we need to research. *Neuropharmacology* **2022**, 109257.

(8) Carhart-Harris, R. L. The entropic brain-revisited. *Neuropharmacology* **2018**, *142*, 167–178.

(9) Petri, G.; Expert, P.; Turkheimer, F.; Carhart-Harris, R.; Nutt, D.; Hellyer, P. J.; Vaccarino, F. Homological scaffolds of brain functional networks. *Journal of The Royal Society Interface* **2014**, *11*, 20140873.

(10) Pallavicini, C.; Vilas, M. G.; Villarreal, M.; Zamberlan, F.; Muthukumaraswamy, S.; Nutt, D.; Carhart-Harris, R.; Tagliazucchi, E. Spectral signatures of serotonergic psychedelics and glutamatergic dissociatives. *NeuroImage* **2019**, *200*, 281–291.

(11) Ly, C.; Greb, A. C.; Cameron, L. P.; Wong, J. M.; Barragan, E. V.; Wilson, P. C.; Burbach, K. F.; Zarandi, S. S.; Sood, A.; Paddy, M. R., et al. Psychedelics promote structural and functional neural plasticity. *Cell Reports* **2018**, *23*, 3170–3182.

(12) Martin, D. A.; Nichols, C. D. The effects of hallucinogens on gene expression. *Behavioral Neurobiology of Psychedelic Drugs* **2017**, 137–158.

(13) McClure-Begley, T. D.; Roth, B. L. The promises and perils of psychedelic pharmacology for psychiatry. *Nature Reviews Drug Discovery* **2022**, *21*, 463–473.

(14) Guiard, B. P.; Di Giovanni, G. *5-ht2a receptors in the central nervous system*; Springer, 2018.

(15) López-Giménez, J. F.; González-Maeso, J. Hallucinogens and serotonin 5-HT 2A receptor-mediated signaling pathways. *Behavioral Neurobiology of Psychedelic Drugs* **2017**, 45–73.

(16) Slocum, S. T.; DiBerto, J. F.; Roth, B. L. Molecular insights into psychedelic drug action. *Journal of Neurochemistry* **2021**,

(17) Olson, D. E. Biochemical mechanisms underlying psychedelic-induced neuroplasticity. *Biochemistry* **2022**, *61*, 127–136.

(18) Aleksandrova, L. R.; Phillips, A. G. Neuroplasticity as a convergent mechanism of

ketamine and classical psychedelics. *Trends in Pharmacological Sciences* **2021**, *42*, 929–942.

(19) Wacker, D.; Wang, C.; Katritch, V.; Han, G. W.; Huang, X.-P.; Vardy, E.; McCorvy, J. D.; Jiang, Y.; Chu, M.; Siu, F. Y. Structural features for functional selectivity at serotonin receptors. *Science* **2013**, *340*, 615–619.

(20) Wang, C.; Jiang, Y.; Ma, J.; Wu, H.; Wacker, D.; Katritch, V.; Han, G. W.; Liu, W.; Huang, X.-P.; Vardy, E. Structural basis for molecular recognition at serotonin receptors. *Science* **2013**, *340*, 610–614.

(21) Wacker, D.; Wang, S.; McCorvy, J. D.; Betz, R. M.; Venkatakrishnan, A.; Levit, A.; Lansu, K.; Schools, Z. L.; Che, T.; Nichols, D. E. Crystal structure of an LSD-bound human serotonin receptor. *Cell* **2017**, *168*, 377–389. e12.

(22) Peng, Y.; McCorvy, J. D.; Harpsøe, K.; Lansu, K.; Yuan, S.; Popov, P.; Qu, L.; Pu, M.; Che, T.; Nikolajsen, L. F. 5-HT2C receptor structures reveal the structural basis of GPCR polypharmacology. *Cell* **2018**, *172*, 719–730. e14.

(23) Kimura, K. T.; Asada, H.; Inoue, A.; Kadji, F. M. N.; Im, D.; Mori, C.; Arakawa, T.; Hirata, K.; Nomura, Y.; Nomura, N. Structures of the 5-HT2A receptor in complex with the antipsychotics risperidone and zotepine. *Nature Structural Molecular Biology* **2019**, *26*, 121–128.

(24) Kim, K.; Che, T.; Panova, O.; DiBerto, J. F.; Lyu, J.; Krumm, B. E.; Wacker, D.; Robertson, M. J.; Seven, A. B.; Nichols, D. E. Structure of a hallucinogen-activated Gq-coupled 5-HT2A serotonin receptor. *Cell* **2020**, *182*, 1574–1588. e19.

(25) Cao, D.; Yu, J.; Wang, H.; Luo, Z.; Liu, X.; He, L.; Qi, J.; Fan, L.; Tang, L.; Chen, Z. Structure-based discovery of nonhallucinogenic psychedelic analogs. *Science* **2022**, *375*, 403–411.

(26) Nichols, D. E. Chemistry and structure–activity relationships of psychedelics. *Behavioral Neurobiology of Psychedelic Drugs* **2017**, 1–43.

(27) Slocum, S. T.; DiBerto, J. F.; Roth, B. L. Molecular insights into psychedelic drug action. *Journal of Neurochemistry* **2021**,

(28) Violin, J. D.; Lefkowitz, R. J. -Arrestin-biased ligands at seven-transmembrane receptors. *Trends in Pharmacological Sciences* **2007**, *28*, 416–422.

(29) Hull, K.; Morstein, J.; Trauner, D. In vivo photopharmacology. *Chemical Reviews* **2018**, *118*, 10710–10747.

(30) Velema, W. A.; Szymanski, W.; Feringa, B. L. Photopharmacology: beyond proof of principle. *Journal of the American Chemical Society* **2014**, *136*, 2178–2191.

(31) Palczewski, K. G protein–coupled receptor rhodopsin. *Annual Review Biochemistry* **2006**, *75*, 743–767.

(32) Morstein, J.; Romano, G.; Hetzler, B.; Plante, A.; Haake, C.; Levitz, J.; Trauner, D. Photoswitchable Serotonins for Optical Control of the 5-HT2A Receptor. *Angewandte Chemie International Edition* **2021**,

(33) Gerwe, H.; He, F.; Pottie, E.; Stove, C.; Decker, M. Enlightening the "Spirit Molecule": Photomodulation of the 5-HT2A Receptor by a Light-Controllable N, N-Dimethyltryptamine Derivative. *Angewandte Chemie International Edition* **2022**, e202203034.

(34) Krylov, A. I.; Gill, P. M. Q-Chem: an engine for innovation. *Wiley Interdisciplinary Reviews: Computational Molecular Science* **2013**, *3*, 317–326.

(35) Frisch, M. J. gaussian09. *http://www. gaussian. com/* **2009**,

(36) Trott, O.; Olson, A. J. AutoDock Vina: improving the speed and accuracy of docking with a new scoring function, efficient optimization, and multithreading. *Journal of Computational Chemistry* **2010**, *31*, 455–461.

(37) O'Boyle, N. M.; Banck, M.; James, C. A.; Morley, C.; Vandermeersch, T.; Hutchison, G. R. Open Babel: An open chemical toolbox. *Journal of Cheminformatics* **2011**, *3*, 1–14.

(38) Wang, C.-D.; Gallaher, T. K.; Shih, J. C. Site-directed mutagenesis of the serotonin 5-hydroxytrypamine2 receptor: identification of amino acids necessary for ligand binding and receptor activation. *Molecular Pharmacology* **1993**, *43*, 931–940.

(39) Zhang, D.; Weinstein, H. Signal transduction by a 5-HT2 receptor: a mechanistic hypothesis from molecular dynamics simulations of the three-dimensional model of the receptor complexed to ligands. *Journal of Medicinal Chemistry* **1993**, *36*, 934–938.

(40) Choudhary, M.; Sachs, N.; Uluer, A.; Glennon, R.; Westkaemper, R.; Roth, B. Differential ergoline and ergopeptine binding to 5-hydroxytryptamine2A receptors: ergolines require an aromatic residue at position 340 for high affinity binding. *Molecular Pharmacology* **1995**, *47*, 450–457.

(41) Almaula, N.; Ebersole, B. J.; Zhang, D.; Weinstein, H.; Sealfon, S. C. Mapping the binding site pocket of the serotonin 5-hydroxytryptamine2A receptor: Ser3. 36 (159) provides a second interaction site for the protonated amine of serotonin but not of lysergic acid diethylamide or bufotenin. *Journal of Biological Chemistry* **1996**, *271*, 14672–14675.

(42) Roth, B.; Shoham, M.; Choudhary, M.; Khan, N. Identification of conserved aromatic residues essential for agonist binding and second messenger production at 5-hydroxytryptamine2A receptors. *Molecular Pharmacology* **1997**, *52*, 259–266.

(43) Shapiro, D. A.; Kristiansen, K.; Kroeze, W. K.; Roth, B. L. Differential modes of agonist binding to 5-hydroxytryptamine2A serotonin receptors revealed by mutation and molecular modeling of conserved residues in transmembrane region 5. *Molecular Pharmacology* **2000**, *58*, 877–886.

(44) Case, D. A.; Aktulga, H. M.; Belfon, K.; Ben-Shalom, I.; Brozell, S. R.; Cerutti, D. S.; Cheatham III, T. E.; Cruzeiro, V. W. D.; Darden, T. A.; Duke, R. E. *Amber 2021*; University of California, San Francisco, 2021.

(45) Lomize, M. A.; Pogozheva, I. D.; Joo, H.; Mosberg, H. I.; Lomize, A. L. OPM database and PPM web server: resources for positioning of proteins in membranes. *Nucleic Acids Research* **2012**, *40*, D370–D376.

(46) Jo, S.; Kim, T.; Iyer, V. G.; Im, W. CHARMM-GUI: a web-based graphical user interface for CHARMM. *Journal of Computational Chemistry* **2008**, *29*, 1859–1865.

(47) Tian, C.; Kasavajhala, K.; Belfon, K. A.; Raguette, L.; Huang, H.; Migues, A. N.; Bickel, J.; Wang, Y.; Pincay, J.; Wu, Q. ff19SB: Amino-acid-specific protein backbone parameters trained against quantum mechanics energy surfaces in solution. *Journal of Chemical Theory and Computation* **2019**, *16*, 528–552.

(48) Gould, I.; Skjevik, A.; Dickson, C.; Madej, B.; Walker, R. Lipid17: A comprehensive AMBER force field for the simulation of zwitterionic and anionic lipids. *Manuscript in preparation* **2018**,

(49) Jorgensen, W. L.; Chandrasekhar, J.; Madura, J. D.; Impey, R. W.; Klein, M. L. Comparison of simple potential functions for simulating liquid water. *The Journal of Chemical Physics* **1983**, *79*, 926–935.

(50) Wang, J.; Wolf, R. M.; Caldwell, J. W.; Kollman, P. A.; Case, D. A. Development and testing of a general amber force field. *Journal of Computational Chemistry* **2004**, *25*, 1157–1174.

(51) McCullagh, M.; Franco, I.; Ratner, M. A.; Schatz, G. C. DNA-based optomechanical molecular motor. *Journal of the American Chemical Society* **2011**, *133*, 3452–3459.

(52) Salomon-Ferrer, R.; Gotz, A. W.; Poole, D.; Le Grand, S.; Walker, R. C. Routine microsecond molecular dynamics simulations with AMBER on GPUs. 2. Explicit solvent particle mesh Ewald. *Journal of Chemical Theory and Computation* **2013**, *9*, 3878–3888.

(53) Darden, T.; York, D.; Pedersen, L. Particle mesh Ewald: An N log (N) method for Ewald sums in large systems. *The Journal of Chemical Physics* **1993**, *98*, 10089–10092.

(54) Ryckaert, J.-P.; Ciccotti, G.; Berendsen, H. J. Numerical integration of the cartesian equations of motion of a system with constraints: molecular dynamics of n-alkanes. *Journal of Computational Physics* **1977**, *23*, 327–341.

(55) Genheden, S.; Ryde, U. The MM/PBSA and MM/GBSA methods to estimate ligand-binding affinities. *Expert Opinion on Drug Discovery* **2015**, *10*, 449–461.

(56) Pottie, E.; Kupriyanova, O. V.; Brandt, A. L.; Laprairie, R. B.; Shevyrin, V. A.; Stove, C. P. Serotonin 2A Receptor (5-HT2AR) Activation by 25H-NBOMe Positional Isomers: In Vitro Functional Evaluation and Molecular Docking. *ACS Pharmacology Translational Science* **2021**, *4*, 479–487.

(57) Johnson, M. P.; Loncharich, R. J.; Baez, M.; Nelson, D. L. Species variations in transmembrane region V of the 5-hydroxytryptamine type 2A receptor alter the structure-activity relationship of certain ergolines and tryptamines. *Molecular Pharmacology* **1994**, *45*, 277–286.

(58) Kao, H.-T.; Adham, N.; Olsen, M. A.; Weinshank, R. L.; Branchek, T. A.; Hartig, P. R. Site-directed mutagenesis of a single residue changes the binding properties of the serotonin 5-HT2 receptor from a human to a rat pharmacology. *FEBS Letters* **1992**, *307*, 324–328.

(59) Nelson, D. L.; Lucaites, V. L.; Audia, J. E.; Nissen, J. S.; Wainscott, D. B. Species differences in the pharmacology of the 5-hydroxytryptamine2 receptor: structurally specific differentiation by ergolines and tryptamines. *Journal of Pharmacology and Experimental Therapeutics* **1993**, *265*, 1272–1279.

(60) Shi, L.; Liapakis, G.; Xu, R.; Guarnieri, F.; Ballesteros, J. A.; Javitch, J. A. 2 Adrenergic Receptor Activation: Modulation of the proline kink in transmembrane 6 by a rotamer toggle switch. *Journal of Biological Chemistry* **2002**, *277*, 40989–40996.

(61) Choudhary, M.; Craigo, S.; Roth, B. A single point mutation (Phe340–> Leu340) of a conserved phenylalanine abolishes 4-[125I] iodo-(2, 5-dimethoxy) phenylisopropylamine and [3H] mesulergine but not [3H] ketanserin binding to 5-hydroxytryptamine2 receptors. *Molecular Pharmacology* **1993**, *43*, 755–761.

(62) Mandado, M.; Hermida-Ramon, J. M. Electron density based partitioning scheme of interaction energies. *Journal of Chemical Theory and Computation* **2011**, *7*, 633–641.

TOC Graphic

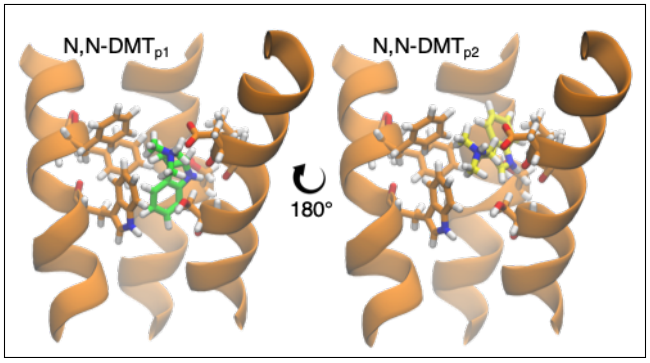

TOC Graphic